Dynamics of Block Copolymer Micelles

Koray Yurekli and Ramanan Krishnamoorti*

Department of Chemical Engineering, University of Houston, Houston, Texas 77204-4004

Received November 19, 2001; Revised Manuscript Received March 1, 2002

ABSTRACT: The structure and melt-state viscoelastic properties for liquidlike ordered micelles, prepared by blending a highly asymmetric polystyrene-rich block copolymer with a polystyrene homopolymer, are examined using a combination of small-angle neutron scattering (SANS), electron microscopy, and dynamic oscillatory rheological measurements. The SANS data, analyzed using a monodisperse Percus−Yevick hard-sphere model, indicated that with homopolymer addition the core diameter remained unchanged while the corona was swollen. The melt viscoelastic data indicated a surprising blend composition-independent "Newtonian" viscosity for blend compositions ranging from 5 to 50 wt % block copolymer. A simple model for the viscosities accounting for the corona swelling, indicated by SANS, provided reasonable agreement with the experimental data.

Introduction

Block copolymers form microphase-separated structures whose geometries and length scales can be tailored by changing the chemical components, volume fraction of the components, and the total degree of polymerization.[1−3] These microphase-separated block copolymers are of significant technological[4] and scientific interest. The technological interest stems from the novel and interesting properties obtained due the presence of the microheterogeneities. Scientifically, they provide model systems for studying a wide range of phenomena including confined polymer chain dynamics,[5] micellization,[6] and polymer reinforcement by fillers. In particular, a blend of homopolymer A with an A-rich A−B or A−B−A block copolymer provides a good dispersion of uniform spherical domains of B in a matrix of A, analogous to a filled polymer or a hard-sphere suspension.[7−9] In the past several years, numerous studies dealing with phase equilibria and microdomain structure[10−14] as well as dynamics[7,8,15−20] of these systems have been pursued.

Watanabe and co-workers have studied micelles of polystyrene−polyisoprene diblock copolymers in low molecular weight polyisoprene matrices[7,8,17,18] and explain the presence of a stable liquidlike dispersion of micelles, in a blend of a homopolymer with an asymmetric diblock, to the screening of the osmotic requirement of the corona blocks by the homopolymer. They conjecture that, once the osmotic requirement for uniform concentration is eliminated, the elastic requirement for randomization results in a liquidlike dispersion. They have also systematically examined the linear and nonlinear viscoelastic properties of block copolymer-based micelles, and by analogy to filled suspensions of silica particles in a polymeric matrix and by direct diffusion measurements, they have elucidated the underlying phenomena responsible for three distinct relaxation processes.[8,17,18] The fast process is attributed to the relaxation of the unentangled matrix polymer, and the intermediate process is thought to arise from the relaxation of the polyisoprene blocks connected to the polystyrene cores. The slow process is attributed to the diffusion of the micelles, which in the case of a dilute dispersion of micelles in an unentangled matrix corresponds to Stokes−Einstein diffusion in the pure matrix. At high concentrations, where the micelles are entangled through their corona blocks, the diffusion is controlled by the viscosity of the blocks, which are estimated from star polymers with the same arm molecular weight. Results from several other groups have corroborated these observations.[16,19] Recently, Zin and co-workers[13] have examined micelle formation in a blend of styrene-rich polystyrene−polyisoprene (SI) diblock with a poly(vinyl methyl ether) (PVME) homopolymer. They have found that micelles with a PI core are dispersed in a PVME matrix with liquidlike order and determined from fitting of small-angle X-ray scattering data that the radius of the PI core is independent of the diblock copolymer concentration.

However, the majority of the blends that have been examined consist of stiff spherical domains in a rubbery matrix such as polystyrene (PS) in a matrix of polyisoprene (PI). The system chosen in this study is the inverse system, consisting of polyisoprene spheres in a polystyrene matrix. This configuration opens up interesting possibilities since it allows fixing of the spherical domains by cross-linking the polyisoprene chains.[21] Also, the asymmetric SI diblock examined here, upon quenching into the ordered region, forms a long-lived metastable phase where the polyisoprene spheres are dispersed with liquidlike order as observed for a number of similar diblocks.[22−24] At a quench depth of 25 °C below the order−disorder temperature (T_{ODT}) of 166 ± 1 °C (determined by SAXS[25]), the ordering half-time is 575 min,[26] which makes it possible to study the disordered micelles even without the addition of a homopolymer. The addition of homopolymer to the diblock copolymer leads to homogeneous blends, and on the basis of prior work, we anticipate that the blends would form liquidlike micelles[10] that persist well above the order−disorder transition.[22,23,27] This paper deals with the structure−property relationships for the uncross-linked blend system, which are both a crucial background for the cross-linked system and because of their importance in understanding properties of multicomponent polymers.

* To whom correspondence should be addressed. E-mail: ramanan@mail.uh.edu.

10.1021/ma012024b CCC: $22.00
Published on Web 04/16/2002

Experimental Section

Materials. The polystyrene−polyisoprene (SI) diblock was prepared by sequential anionic polymerization and is 90 wt % PS with a total weight-average molecular weight (M_w) of 65 100 and a polydispersity index $M_w/M_n < 1.06$.[22,23,26] The PS homopolymer used in the study was obtained from Polymer Source and had a M_w of 90 000 and a $M_w/M_n < 1.04$. Samples with SI weight fraction (w_{SI}) of 0.05, 0.20, 0.30, and 0.50 were prepared in the following way: The appropriate amounts of PS and the SI diblock were dissolved in tetrahydrofuran (THF). The resulting solution was left to dry in a fume hood overnight. Once the bulk of the THF was evaporated, the samples were completely dried in a vacuum oven at room temperature, followed by heating at ∼100 °C for 6 h.

Small-Angle Neutron Scattering. Small-angle neutron scattering (SANS) samples were prepared in a vacuum mold to achieve uniform, bubble-free samples. Appropriate quantities of the blend were placed in the annulus of a brass washer with outer diameter of 25 mm, an inner diameter of 15 mm, and thickness of 1 mm and compression-molded in a heated vacuum mold at a temperature of 160 °C. Prior to SANS measurements, the sample (in the brass annulus) was sandwiched between quartz windows. SANS measurements were performed on the 30 m SANS beamline (NG3) at NIST, Gaithersburg, MD. Neutrons with wavelength (λ) of 6 Å and $\Delta\lambda/\lambda$ of 0.15 were used with sample-to-detector distances ranging from 5 to 6.5 m. The SANS spectra were reduced and corrected for background scattering.[28] Absolute cross sections were obtained with the use of a silica gel secondary standard. Finally, a q-independent incoherent scattering correction was subtracted prior to data analysis.[28] The incoherent scattering calculations were based on the scattering from a purely protonated homopolymer and the proton density of the studied samples. The SANS data were analyzed using both a paracrystalline body-centered-cubic (bcc) model and the Percus−Yevick hard-sphere liquid theory, and these are discussed below with the data.

Transmission Electron Microscopy. Transmission electron microscopy (TEM) samples were microtomed from bulk blend samples with $w_{SI} = 0.05$, 0.20, 0.30, and 0.50 and stained with OsO_4 vapor. The microscopy was done using a Phillips EM 300 TEM operated at 160 keV.[29] Images were taken at magnifications of 10 000×, 20 000×, 25 000×, and 50 000×. The collected pictures were cleaned, reduced to binary images using thresholding, and analyzed for particle sizes and interparticle distances with a commercially available image analysis software.

Linear Viscoelasticity. Samples for linear viscoelastic measurements were prepared by vacuum-molding at ∼135 °C for 2 h. The resulting pellets were about 1−2 mm thick with a diameter of 25 mm. Viscoelastic measurements were carried out in a Rheometrics ARES melt-state rheometer with a transducer operating over a range of 0.2−2000 g cm and over a frequency (ω) range of 0.001−100 rad/s. Constant strain amplitude (γ_0) frequency sweeps were performed using a 25 mm parallel plate geometry. A sinusoidal strain of the form $\gamma(t) = \gamma_0 \sin(\omega t)$ was applied, and the resulting measured stress was converted to the in-phase storage modulus (G') and the out-of-phase loss modulus (G''). The phase angle, tan δ, and the complex viscosity, η^*, were calculated using the definitions $\tan\delta = G''/G'$ and $\eta^* = (1/\omega)[(G')^2 + (G)''^2]^{0.5}$. The frequency sweeps were carried out as a function of temperature between 130 and 160 °C. Because of the nonlinearity of the viscoelasticity at higher strains, all experiments were performed using as small strain amplitudes as possible. The strain amplitudes varied from 2.5×10^{-4} to 0.3 depending on temperature and frequency.

Results and Discussion

Small-Angle Neutron Scattering. The coherent neutron scattering intensities for the diblock and the blends as a function of q (= $(4\pi/\lambda)\sin\theta$) in the melt state at 135 °C are shown in Figure 1. A relatively strong first maximum at $q \sim 0.026$ Å^{-1} and a weak shoulder at $q \sim 0.04$ Å^{-1} are the main features for scattering from the SI diblock copolymer. Similar features, albeit at lower q values and with lower intensities, are observed for the blends with $w_{SI} = 0.20$, 0.30, and 0.50. For the blend with $w_{SI} = 0.05$, however, no discernible SANS peaks are observed in the q range measured. We also note that the data at 170 °C are similar to the data at 135 °C with lower intensity in all cases. Further, the SANS measurements described here were performed on unlabeled polymers and exploit the natural neutron scattering contrast between polyisoprene and polystyrene,[30] and that is responsible for the low-intensity values. Last, the lack of a sharp upturn in the lowest q region indicates that the system is compatible, and no partial demixing or macrophase separation occurs. Macroscale phase separation between the diblock and the homopolymer might be expected on the basis that the matrix PS chains are of higher chain length than the corona PS. However, the relatively small differences in molecular weight between the corona and the matrix chains allows for their compatibility.

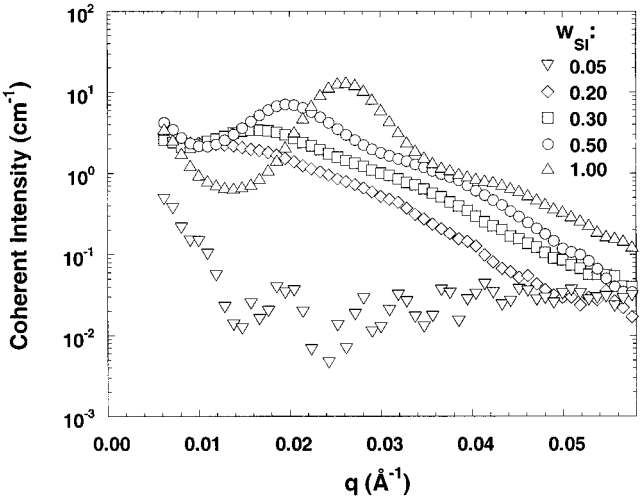

Figure 1. Absolute coherent cross sections for the SI diblock and the blends as a function of q (= $(4\pi/\lambda)\sin\theta$) in the melt state at 135° C shown in a semilog plot for clarity. Note the first maximum at $q \sim 0.026$ Å^{-1} and a weak shoulder at $q \sim 0.04$ Å^{-1} for the SI diblock copolymer. Peak positions and intensities decrease with decreasing SI content. For the sample with $w_{SI} = 0.05$, the peak intensities are too small for analysis.

As noted in the Introduction, previous studies by Register and co-workers have shown that the ordering half-time of this particular SI diblock copolymer is 575 min at 140 °C.[26] The SANS measurements described in Figure 1 were undertaken within 2 h after cooling below T_{ODT}, allowing the study of liquidlike ordering of micelles. The lack of well-defined higher-order peaks in the diblock and the blends suggests that the PI microdomains are dispersed with a liquidlike order rather than being positioned on a paracrystalline lattice. Similar thermal protocols were also adopted for the TEM and viscoelasticity studies, ensuring liquidlike order in all cases.

The invariant (= $\int_0^\infty q^2 I(q)\,dq$) for the $w_{SI} = 0.20$, 0.30, and 0.50 blends, calculated on the basis of the scattering data at 135 °C, decreases with decreasing SI content, and an extrapolation of the invariant to zero suggests a critical micelle concentration (cmc) of $w_{SI} = 0.06 \pm 0.01$. This assignment of the cmc is consistent with the

Table 1. bcc Lattice Parameters from SANS Data

$w_{SI} = 0.30$			$w_{SI} = 0.50$		
R (Å)	D (Å)	a (Å)	R (Å)	D (Å)	a (Å)
89	476	549	86	388	448

scattering signatures observed for the $w_{SI} = 0.05$ blend in Figure 1, where no features such as scattering peaks are observed in the measured q range.

We apply a Percus−Yevick (PY)-based liquid model to analyze the SANS data presented in Figure 1. However, as a first approximation, a bcc lattice model was applied to obtain interdomain distances and domain sizes for the spherical PI domains. Previous studies have indicated that the ordering of the domains onto a paracrystalline lattice does not appreciably change the location of the first scattering maximum;[31] this allows us to use the interdomain distances and domain sizes from such a fitting as good initial guesses in the PY model (described below). The lattice parameters R (radius of the PI microdomain), D (nearest-neighbor distance between microdomains), and a (the length of the side of the unit cell) are calculated from the position of the first maximum, q^*, and the isoprene volume fraction, ϕ_I, using the following relationships for the bcc lattice model:[24]

$$R = (2\pi/q^*)(3\phi_I/\sqrt{8}\pi)^{1/3}$$
$$D = \sqrt{6}\pi/q^*$$
$$a = \sqrt{8}\pi/q^* \quad (1)$$

Values of R, D, and a based on the bcc lattice model are tabulated in Table 1.

However, a more realistic model for these systems is to consider them as a dispersion of hard spheres with liquidlike order. Since the interparticle distances are on the order of the particle sizes, both intraparticle and interparticle interferences are taken into account when modeling the SANS intensity. The total coherent intensity is written as

$$I(q) = \epsilon K P(qR_I)\, S(q) \quad (2)$$

where K is the contrast factor between the polyisoprene core and the polystyrene matrix, ϵ is an adjustable parameter accounting for intermixing of the core and matrix and the consequent reduction in scattering contrast, $P(qR_I)$ is the intraparticle structure factor, and $S(q)$ is the interparticle structure factor. The monodisperse intraparticle interference function $P(qR_I)$ is characterized by R_I, the isoprene sphere radius (equivalent to R in the bcc model), and v_I, the isoprene sphere volume, and is given by

$$P(qR_I) = \left(v_I \frac{3}{(qR_I)^3}[\sin(qR_I) - qR_I \cos(qR_I)]\right)^2 \quad (3)$$

The interparticle interference, which results in the main peak of the SANS spectra, is modeled by the structure factor, $S(q)$, related to the Fourier transform of the PY pair correlation function for hard spheres.[31−34] The PY model has been widely used to study systems with liquidlike order because it approximately accounts for the correlations between hard-sphere particles resulting from the interparticle interactions and is reliable even at large particle densities.[32] The resulting structure factor $S(q)$ is[31−33]

$$S(q) = \left(1 + 24 v_{hs} \frac{G(x)}{x}\right)^{-1} \quad (4)$$

where $x = 2qR_{hs}$ and

$$G(x) = \frac{\alpha}{x^2}(\sin x - x\cos x) + \frac{\beta}{x^3}(2x \sin x + (2 - x^2)\cos x - 2) + \frac{\gamma}{x^5}(-x^4 \cos x + 4[(3x^2 - 6)\cos x + (x^3 - 6x)\sin x + 6]) \quad (5a)$$

$$\alpha = (1 + 2v_{hs})^2/(1 - v_{hs})^4 \quad (5b)$$

$$\beta = -6v_{hs}(1 + v_{hs}/2)^2/(1 - v_{hs})^4 \quad (5c)$$

$$\gamma = (1/2)v_{hs}(1 + 2v_{hs})^2/(1 - v_{hs})^4 \quad (5d)$$

R_{hs} and v_{hs} refer to the hard-sphere radius and the hard-sphere volume, respectively. The hard sphere is defined by the range of repulsive interaction between spheres; therefore, it is larger than R_I and can be thought to include the PI core and the PS corona. The PS corona is included in the hard sphere because being covalently bonded to the core PI, the PS chains contribute to the steric interactions between particles. The PY fits to the scattering from the blends with $w_{SI} = 0.30$ and 0.50 at 135 °C, shown in Figure 2, were achieved by varying four parameters, R_I, R_{hs}, v_{hs}, and ϵ, in a nonlinear least-squares fitting scheme with eqs 2−5. The prefactor ϵ (≤ 1), which decreases with increasing PS content, was necessary because the contrast between the micelles, which contain the PS corona and the matrix, was less than K, the calculated contrast between PI and PS. Finally, as seen in Figure 2b, the quality of the PY fit becomes quite poor at high q values. This is presumably due to the low coherent scattered intensities (with large errors) at high q values resulting from the weak natural contrast between PS and PI and the crude subtraction of the incoherent scattering resulting from the hydrogen atoms present in the scattering volume. Thus, the data at high q are unable to rigorously verify that the PY model provides accurate fitting and that in fact the micelles are arranged in a liquidlike disorder. Nevertheless, the reasonable agreement at low q and the accompanying TEM data provide reasonable confidence for the presence of liquidlike micelles.

The values of R_I, R_{hs}, and v_{hs} obtained are shown in Figure 3. The most important observation is that while R_I is almost independent of w_{SI}, R_{hs} increases with increasing added homopolymer. These observations are in good agreement with those of Gohr et al.[19] and Ahn et al.[13] where they examined the formation of micelles in high molecular weight homopolymers and polymer blends, respectively. The increase in R_{hs} is similar to that observed for partially wet-brush systems where the homopolymer dissolves poorly in the corona.[19] The constancy of the R_I value would suggest a relatively invariant aggregation number for the micelles. Finally, v_{hs} monotonically increases with increasing diblock concentration and expected based on the increasing isoprene content and the strong repulsion between PS and PI.[1,22]

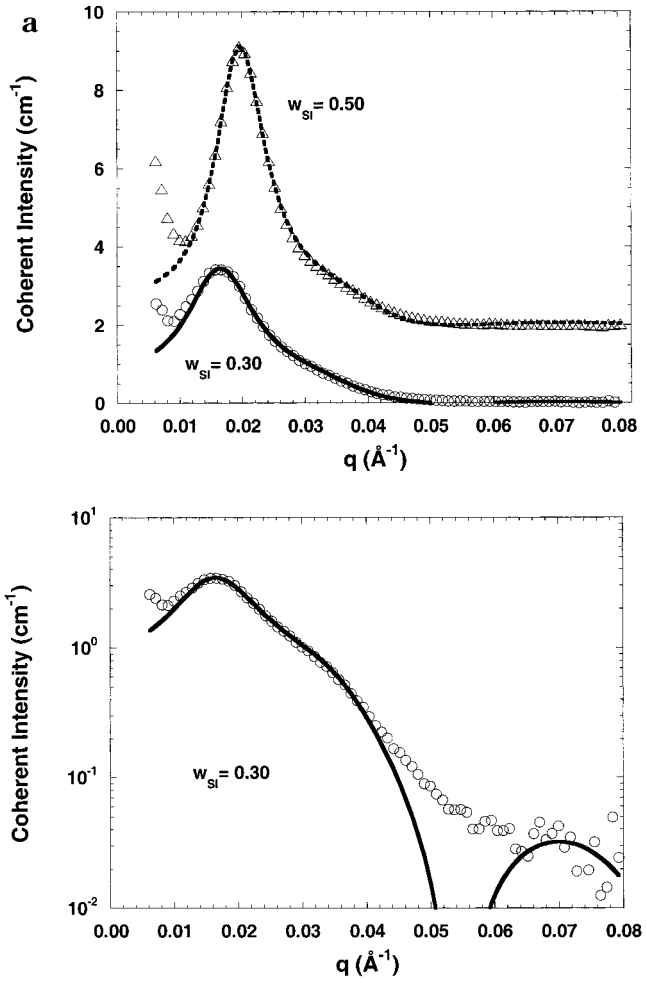

Figure 2. Fits of the SANS absolute coherent cross sections using the monodisperse Percus−Yevick interparticle correlation function. **(**a**)** For blends with $w_{SI} = 0.30$ and 0.50 shown in linear intensity scale. The data for the $w_{SI} = 0.50$ blend is shifted vertically 2 cm^{-1} for clarity. **(**b**)** For the blend with $w_{SI} = 0.30$ shown on a logarithmic intensity scale.

Transmission Electron Microscopy. TEM images of the blend with $w_{SI} = 0.50$ at magnifications of 10 000×, 20 000×, and 50 000× as well as 20 000× magnification images for the blends with $w_{SI} = 0.20$ and 0.30 are shown in Figure 4. These are representative snapshots of the structure in the sample and corroborated by several (tens of) images taken at different locations and magnifications. Samples were prepared by rapidly quenching the samples to room temperature following their equilibration at 135 °C. Because of the high glass transition temperature of the PS matrix (100 °C), we anticipate that the structure remains unaltered following the quench and is in fact representative of the melt-state structure. An OsO_4 stain was used, leading to a preferentially staining of the unsaturated PI units.[35]

Not surprisingly, in these blends, roughly spherical micellar microdomains of PI are observed in a PS matrix. Furthermore, the spherical micelles do not reveal a lattice superstructure but are dispersed with liquidlike order. These observations are in good agreement with the SANS results discussed above. Further, like the SANS results, the TEM images do not reveal any indication of macrophase separation. The nanometer-scale inhomogeneties observed are attributed to staining or digitizing artifacts in the micrographs. Since these artifacts were on the order of the microdomain size scale, they precluded us from performing quantitative data analysis of the images for size distributions and micellar dispersion.

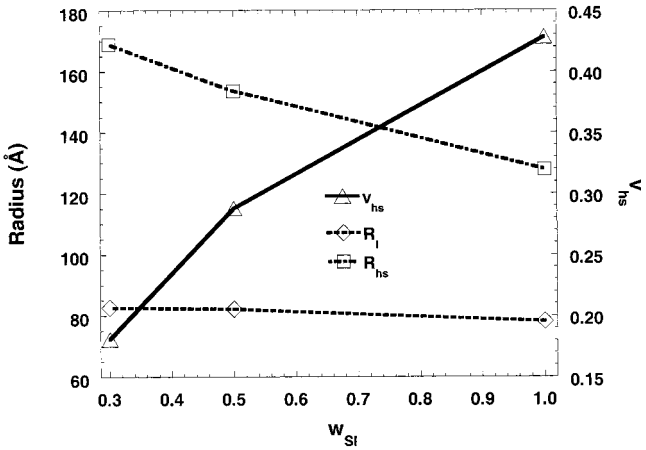

Figure 3. Results of the Percus−Yevick (PY) fit to the SANS data as a function of the SI diblock copolymer weight fraction. The radius of the PI core, R_I, is nearly constant, but the hard-sphere radius, R_{hs}, decreases almost linearly with increasing w_{SI}. The lines are included merely as a guide to the eye and do not represent a fit to the data.

Thus, both scattering measurements and electron microscopy suggest that the blends of the SI block copolymer and PS homopolymer form micelles with liquidlike ordering with no macroscale phase separation. Simple mean-field incompressible random phase approximation based calculations suggest a significant lowering of the order−disorder transition temperature with homopolymer addition and imply disordered liquidlike behavior for the blends examined here.[2,36] Self-consistent theories suggest that even in symmetrical systems the addition of low molecular weight homopolymers can lead to an increase in the order−disorder transition temperature.[12,37,38] Previous experiments on mixtures of symmetrical block copolymers and homopolymers (both low and high molecular weight) and mixtures of asymmetrical block copolymers with low molecular weight homopolymers can lead to significant stabilization of the ordered states.[10,14,39] However, in the measurements described here, the blends do not show clear signatures for the presence of ordered microdomains. In fact, recent experiments by Han and coworkers[14,27,40] and Lodge et al.[38,41] have suggested the existence of liquidlike micelles at temperatures significantly higher than the order−disorder transition temperature. The structural results presented here are consistent with those findings and indicative of liquidlike micellar structures.

Linear Viscoelasticity. Melt-state viscoelastic master curves for the PS homopolymer ($w_{SI} = 0$) and SI block copolymer ($w_{SI} = 1$) are shown in Figures 5 and 6, respectively. The data gathered at temperatures between 130 and 160 °C have been shifted to a common reference temperature (T_0) of 130 °C using the principle of time−temperature superposition. Horizontal (frequency) as well as vertical (modulus) shifts (a_T and b_T, respectively) have been used to achieve superposition of the data. The values of b_T varied from 0.9 to 1.1 and are consistent with calculations based on changes in density with temperature. On the other hand, the values of a_T are nearly independent of w_{SI} and obeyed the WLF equation as discussed below.

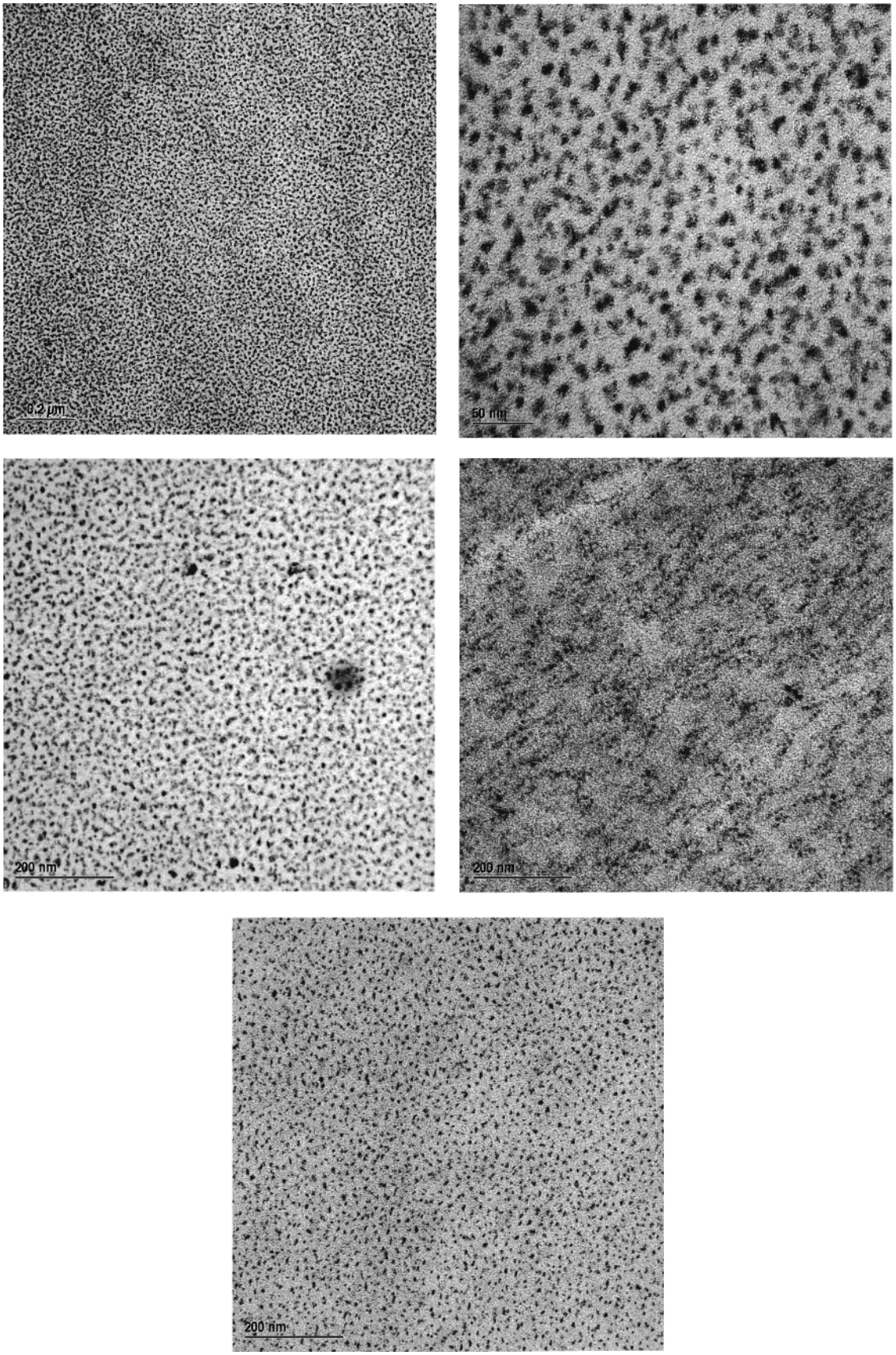

Figure 4. TEM images at various magnifications of several PS−SI blend compositions: **(a)** $w_{SI} = 0.50$, 10 000×; **(b)** $w_{SI} = 0.50$, 20 000×; **(c)** $w_{SI} = 0.50$, 50 000×; **(d)** $w_{SI} = 0.20$, 20 000×; **(e)** $w_{SI} = 0.30$, 20 000×. The dark regions are regions of higher electron density and correspond to the OsO_4-stained polyisoprene units. These images show a liquidlike dispersion of spherical PI cores in a PS matrix and are representative of all micrographs taken at different locations and magnifications.

The homopolymer PS behaves as expected from a monodisperse entangled polymer with a plateau region at high frequencies, a crossover of G' and G'' corresponding to chain relaxation (with a longest relaxation

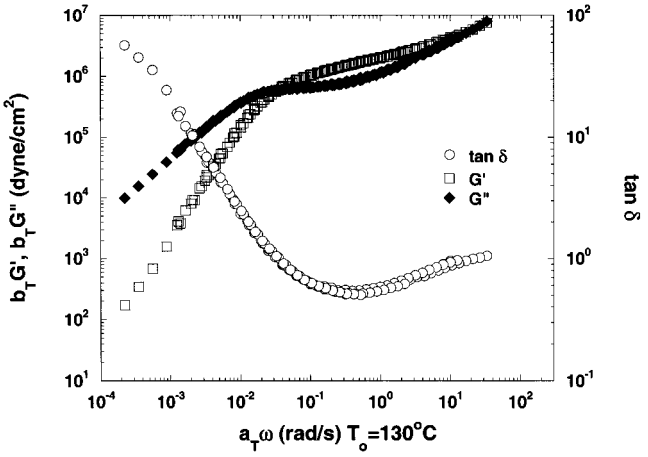

Figure 5. Time−temperature superposed linear viscoelastic master curve for the PS homopolymer with a reference temperature (T_0) of 130 °C. The viscoelastic response is characteristic of a well-entangled polymer with a crossover frequency (ω_c) of ∼0.03 rad/s below which liquidlike relaxation is observed. The frequency shift factors (a_T) are shown in the inset to Figure 9, and the modulus shift factors (b_T) ranged from 0.9 to 1.1.

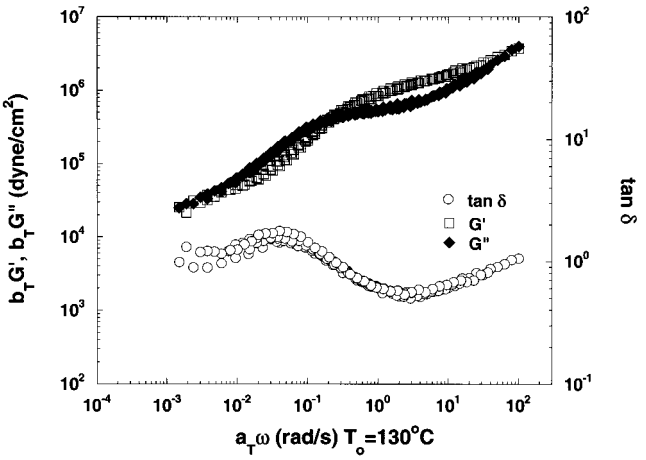

Figure 6. Time−temperature superposed linear viscoelastic master curve for the SI diblock copolymer with a reference temperature T_0 of 130 °C. The crossover frequency (ω_c) of ∼0.2 rad/s corresponds to the relaxation of the PS block. Note the weak frequency dependence of G' in the low-frequency region showing the absence of terminal relaxation in the frequency range examined.

time of 200 s at 130 °C) and liquidlike terminal behavior at low frequencies. For the SI block copolymer the high-frequency behavior and behavior down to the crossover of G' and G'' (corresponding to a relaxation time of 30 s at 130 °C) are similar to that of the PS homopolymer. This relaxation time is presumed to correspond to the relaxation of the PS corona chains and is consistent with the lower molecular weight of the block copolymer. However, at low frequencies the SI block copolymer exhibits nonterminal behavior. The storage modulus G' shows a weak dependence on ω and is consistent with that of a material with structural disorder and not akin to that exhibited by cubic lattice ordered spherical microdomains.[17,42] There are at least two possible mechanisms for slower relaxations that would shift the terminal behavior to lower frequencies. One is the diffusion of complete chains, hampered by the trapping of the PS−PI junction point at the interface of the microdomains as suggested by Register and co-workers.[22] Another is diffusion of the micelles, which can

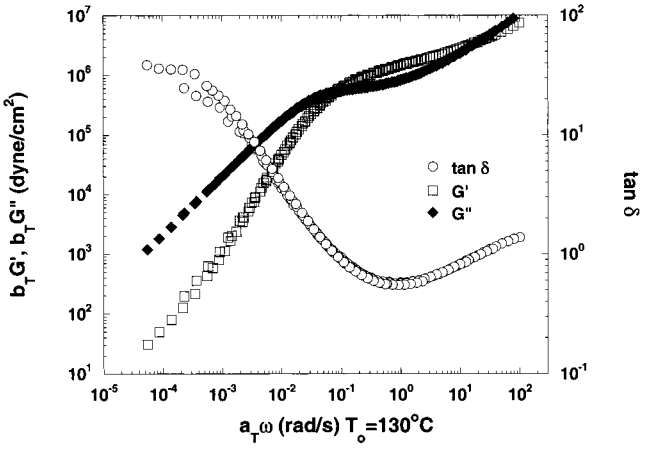

Figure 7. Time−temperature superposed linear viscoelastic master curve for the blend with $w_{SI} = 0.30$. Note the similarity in features to the PS homopolymer response. The crossover frequency (ω_c) of ∼0.1 rad/s corresponds to the relaxation of the PS chains. The relaxation time is representative of all blends (Table 2) and lies between that of the PS homopolymer and the SI diblock copolymer.

have some cooperative character resulting from interparticle interactions present at high concentrations of micelles.[8,17,18]

As shown in Figure 7, the viscoelastic behavior of the blend with $w_{SI} = 0.30$ resembles that of the pure PS (with $G'' \propto \omega$ and $G' \propto \omega^2$) and is representative of the response of the blends with $w_{SI} < 0.50$. Previous studies by Watanabe and co-workers have demonstrated that the linear viscoelastic results for PS spheres in a PI matrix exhibit three relaxation processes—the fastest corresponding to the relaxation of the homopolymer matrix, the intermediate relaxation corresponding to the relaxation of the corona PI chains, and the slowest process corresponding to the diffusion of the spherical micelles.[8,17] In the present study, where the molecular weight of the matrix is larger than the PS corona, only one relaxation process is observed and is attributed to the relaxation of the polystyrene matrix and corona chains. This conclusion is based on the fact that time−temperature superposition works and, as detailed below, on the agreement of the frequency shift factors with those for the homopolymer PS. If the PI block relaxations contributed significantly to the observed moduli, a breakdown of the time−temperature superposition would be expected due to the differences in the temperature dependence of the relaxations of PS and PI (with the expectation that PS and PI exhibit distinct relaxation and temperature dependences of relaxation) and due to the changes in the sharpness of the PS/PI interphase with temperature. Diffusion times for the micelles, calculated using the Stokes−Einstein relationship with values of hydrodynamic diameters from SANS measurements and matrix viscosity from linear viscoelastic measurements on PS, suggest a relaxation time of 1.2×10^5 s at 130 °C for a blend with 50% added homopolymer. The combination of long relaxation time and relatively low values of the moduli at these long times does not allow us to investigate the relaxation of the micelles via linear relaxation measurements. Therefore, only the faster relaxation, which is attributed to the PS chains, is observed and discussed.

The PS chain relaxation time, as deduced from the crossover frequency in Figure 7, is shorter for the $w_{SI} = 0.30$ blend than for the pure PS sample. In fact, as

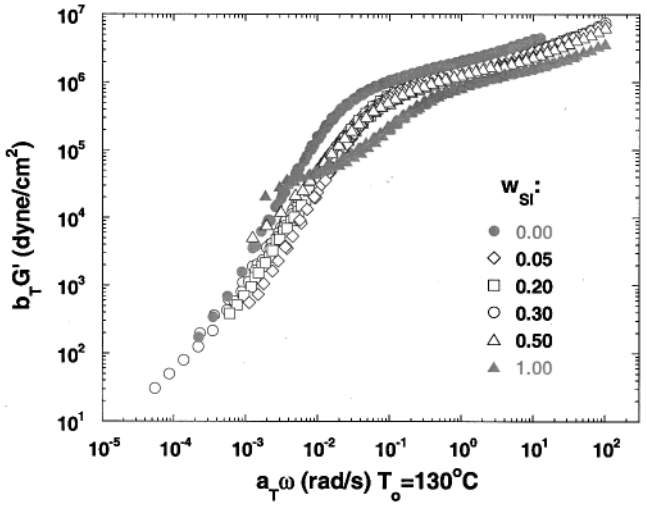

Figure 8. Time−temperature superposed storage modulus (G') master curves (with a common T_0 = 130 °C) for the homopolymer PS, SI diblock copolymer, and all blends. The PS chain relaxation times for the blends, as deduced from the downturn in G' at intermediate frequencies, are nearly independent of w_{SI} and lie between the values for the PS homopolymer and the SI diblock copolymer. The vertical shift factors (b_T) employed for the superpositioning lie between 0.9 and 1.1, and the horizontal shift factors (a_T) are shown in the inset of Figure 9.

Table 2. Crossover Frequencies of G' and G'' at 130 °C

SI wt fraction (w_{SI})	0	0.05	0.20	0.30	0.50	1.00
crossover freq (ω_c)	0.032	0.100	0.090	0.085	0.090	0.221

seen in Table 2, the crossover frequencies for the blends (which span a w_{SI} range of 0.05−0.50) are almost independent of w_{SI} and lie between those of PS and the SI diblock. Similar trends are also observed for G' (Figure 8) and η^* (Figure 9)[43] of the blends. The addition of diblock to PS results in a speeding up of the relaxation of the PS chains or equivalently decreasing η^*. Consistent with the blend composition dependence of the crossover frequency, the low-frequency ("Newtonian") viscosity is also independent of the blend composition. The most intriguing aspect of the data is the large influence observed on the viscoelastic functions with the addition of only 5 wt % of the diblock copolymer and the subsequent invariance of the viscoelastic properties with additional diblock copolymer. Our explanations for some of these features are discussed below.

In Figure 8 for the blend with w_{SI} = 0.50, the low-frequency dependence of G' displays departure from terminal liquidlike behavior. This can be explained by an increase in the fraction of chains containing trapped junction points and also by an increase in the cooperativity of motion with increasing micelle concentration. In fact, at such high concentrations of the diblock the coronas of individual micelles might be expected to interpenetrate, resulting in a higher degree of cooperativity than simple percolation of hard spheres.[44] However, even for this blend, the viscous component G'' exceeds G' and exhibits liquidlike character as observed in Figure 9.

On the other hand, the temperature dependence of the values of a_T, shown as an inset in Figure 9, indicates that the shift factors for all samples, including the SI diblock copolymer and PS homopolymer, are within the errors of the measurement identical, indicating the small influence of polyisoprene on the dynamics in these systems. The WLF coefficients ($\log a_T = -[(c_1(T - T_0)]/(T - T_0 + c_2)$) with $c_1 = 9.6$, $c_2 = 96$ K, and $T_0 = 403$ K are in reasonable agreement with previous studies by Plazek[45] and Graessley[46] on polystyrenes.

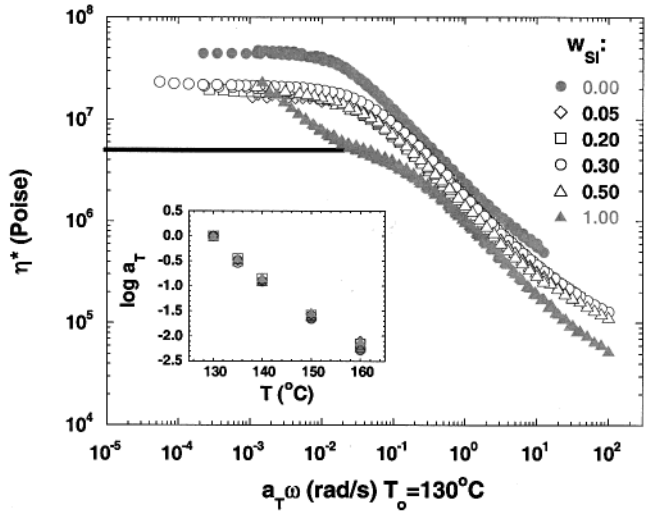

Figure 9. Time−temperature superposed complex viscosity (η^*) master curves (with a common T_0 = 130 °C) for the homopolymer PS, SI diblock copolymer, and all blends. For the blends, the curvature in the η^* values from the power-law regime to the zero shear value is less sharp as compared to the homopolymer PS. This is probably due to the bimodal distribution of molecular weights for PS in the blends.[43] The zero shear viscosities for the blends are nearly independent of w_{SI} and lie between the values for the PS homopolymer and the SI diblock copolymer. For the SI diblock copolymer, the zero shear viscosity of the PS blocks is estimated as shown in the figure. The inset shows that the frequency shift factors (a_T) are nearly identical for all samples.

The surprising composition-independent low-frequency viscosity for the blends (Figure 9) deserves closer attention. It would be expected that addition of diblock copolymer to the homopolymer and the consequent formation of micelles would lead to an increase in the viscosity due to the junction point trapping. However, the observed viscosities of the blends are lower than that of the PS homopolymer and independent of the amount of SI added. We attempt to explain these observations, at least for the relatively high SI content mixtures, with a simple model that assumes the incorporation of some PS homopolymer chains into the coronas of the spherical micelles. On the basis of the SANS measurements and their interpretation in terms of the PY model, we infer that the coronas are swollen by the incorporation of matrix chains. Since the molecular weight of the PS block in the diblock is smaller than the PS homopolymer, a decrease in the viscosity of the corona swelling PS would be anticipated through a dilution of entanglements. By neglecting chain stretching and assuming a sharp interface between the corona and the matrix, the validity of this model can be verified for the w_{SI} = 0.30 and 0.50 blends, which have discernible SANS peaks, by using the following mixing rules:

$$\eta^*_{\text{blend}} = \phi_{\text{matrix}}\eta^*_{\text{matrix}} + \phi_{\text{corona}}\eta^*_{\text{corona}} \tag{6}$$

$$\eta^*_{\text{corona}} = \phi_1{}^2\eta_1^* + \frac{4(G^0_{N,1})^{1/2}(G^0_{N,2})^{1/2}\phi_1\phi_2}{\dfrac{G^0_{N,1}}{\eta_1^*} + \dfrac{G^0_{N,2}}{\eta_2^*}} + \phi_2^2\eta_2^* \tag{7}$$

where $G^0_{N,1}$ and $G^0_{N,2}$ are the plateau moduli for the

matrix PS and the PS block of the diblock and are assumed to have the same value resulting in the simplification of eq 7 to

$$\eta^*_{corona} = \phi_1^2\eta^*_1 + \frac{4\phi_1\phi_2}{\frac{1}{\eta^*_1} + \frac{1}{\eta^*_2}} + \phi_2^2\eta^*_2 \qquad (8)$$

$\eta^*_1 = \eta^*_{matrix}$ and represents the complex viscosity of the PS homopolymer, η^*_2 is the PS block viscosity in the SI diblock (estimated from linear viscoelastic measurements in Figure 9), and η^*_{blend} is the observed low-frequency "Newtonian" viscosity for the blend, assumed to be entirely due to PS since the PI is well above it glass transition temperature. The PS volume fractions in the matrix and the corona are labeled as ϕ_{matrix} and ϕ_{corona}, respectively. On the other hand, ϕ_1 and ϕ_2 represent the volume fraction in the corona of homopolymer PS and block PS, respectively. Equation 6 assumes that in the blends the corona and matrix are only weakly interacting, thus suggesting the simple volume fraction weighted addition of the viscosity of the corona and the matrix. Furthermore, any effect of the interpenetration of the coronas of the micelles on viscosity is ignored. On the other hand, the viscosity of the PS corona is modeled by eq 8 and employs a simple mixing rule developed for a mixture of two monodisperse entangled polymers using the double reptation model.[47] Although more sophisticated models that account for the changes in the contributions of constraint release and tube dilation upon blending of two homopolymers are available,[48] there is no established method to take into account the effects introduced by the PS−PI junctions in our blend system. Moreover, the similar molecular weights of the matrix and the corona PS should result in only small differences to the constraint release corrections, implying that the simple double reptation model should serve as an adequate first approximation.

Using eqs 6 and 8, the expected viscosities from the swelling of the corona diameter determined by the PY fit of the SANS data are calculated. For the blends with $w_{SI} = 0.30$ and 0.50, the corona diameters are swollen by factors of 2.6 and 1.9, respectively, and resulting in blend viscosities of 2.8×10^7 and 1.9×10^7 P, respectively. Experimentally, these viscosities are 1.9×10^7 and 1.95×10^7 P, respectively. While being quantitatively inconsistent, the predicted viscosities are significantly lower than the PS homopolymer viscosity and do not depend strongly on SI diblock content. The discrepancies between the calculated and experimentally measured values can be due to the simplistic mixing rules used or the inaccuracy in the estimation of the PS block viscosity in the SI diblock or the use of a monodisperse intraparticle interference function for modeling the SANS data. Further, the assumption that $G^0_{N,1} = G^0_{N,2}$ may not be correct due to the trapping of the corona chains at the PS−PI junctions as well as the presence of free PS−PI chains not incorporated into micelles, which make up approximately 6 wt % (estimated from the critical micelle concentration) of the total diblock in the blend. Perhaps incorporation of more sophisticated viscoelastic models to describe the matrix/core−shell system[20,49] and to describe the blending in the corona might lead to better quantitative agreement between experiments and theory.

Concluding Remarks

The viscoelasticity of mixtures of a highly asymmetrical diblock SI copolymer with a homopolymer PS of higher molecular weight than the block PS revealed a highly unusual behavior for the relaxation times and the low-frequency viscosity. Structural probes of in-situ SANS and ex-situ TEM lend credence to a liquidlike micellar structure whose aggregation number was unchanged with homopolymer dilution and whose corona was increasingly swollen with homopolymer incorporation. These structural features are integrated with a simple mixing model to describe the observed viscosity behavior and reasonable qualitative agreement, at least for the blends with high diblock fraction, between theory and experiment is observed. It must be noted that the blend with $w_{SI} = 0.05$ has little or no micellar structure, and we are still trying to understand the dramatic difference between the viscosity of this blend and the pure PS. Further, the lack of quantitative agreement between the experimental and the theoretical model for the other blends ($w_{SI} = 0.20$, 0.30, and 0.50) could result from the neglecting of chain stretching and the assumption of sharp interfaces between corona and matrix and from the relatively simplistic mixing rules applied. At least some of these assumptions might be better satisfied for higher molecular weight block copolymers and matrix chains, and these are in fact experiments we are currently pursuing.

Acknowledgment. The authors thank Prof. Register for generously sharing the block copolymer and valuable characterization information. Useful discussions with Prof. Watanabe are also gratefully acknowledged. We thank the National Science Foundation (DMR-9875321) and ExxonMobil Chemical Company for funding this research. The SANS measurements conducted at NIST were supported by the National Science Foundation under Agreement DMR-9986442. Finally, we acknowledge the reviewers of this manuscript for valuable suggestions regarding the viscoelastic model presented here.

References and Notes

(1) Khandpur, A. K.; Forster, S.; Bates, F. S.; Hamley, I. W.; Ryan, A. J.; Bras, W.; Almdal, K.; Mortensen, K. *Macromolecules* **1995**, *28*, 8796−8806.
(2) Leibler, L. *Macromolecules* **1980**, *13*, 1602−1617.
(3) Mortensen, K.; Almdal, K.; Schwan, D.; Bates, F. S. *J. Appl. Crystallogr.* **1997**, *30*, 702−707.
(4) Allen, C.; Yu, Y.; Maysinger, D.; Eisenberg, A. *Bioconjugate Chem.* **1998**, *9*, 564−572.
(5) Floudas, G.; Meramveliotakim, K.; Hadjichristidis, N. *Macromolecules* **1999**, *32*, 7496−7503.
(6) Forster, S.; Zisenis, M.; Wenz, E.; Antonietti, M. *J. Chem. Phys.* **1996**, *104*, 9956−9970.
(7) Watanabe, H.; Yao, M.-L.; Sato, T.; Osaki, K. *Macromolecules* **1997**, *30*, 5905−5912.
(8) Watanabe, H.; Sato, T.; Osaki, K.; Hamersky, M. W.; Chapman, B. R.; Lodge, T. P. *Macromolecules* **1998**, *31*, 3740−3742.
(9) Watanabe, H.; Kotaka, T. *Polym. J.* **1983**, *15*, 337−347. Watanabe, H.; Kotaka, T.; Hashimoto, T.; Shibayama, M.; Kawai, H. *J. Rheol.* **1982**, *26*, 153. Watanabe, H.; Kotaka, T. *Polym. J.* **1982**, *14*, 739. Watanabe, H.; Kotaka, T. *J. Rheol.* **1983**, *27*, 223.
(10) Winey, K. I.; Thomas, E. L.; Fetters, L. J. *Macromolecules* **1992**, *25*, 2645−2650. Winey, K. I.; Thomas, E. L.; Fetters, L. J. *J. Chem. Phys.* **1991**, *95*, 9367−9375.
(11) Han, C. D.; Baek, D. M.; Kim, J.; Kimishima, K.; Hashimoto, T. *Macromolecules* **1992**, *25*, 3052−3067.
(12) McConnell, G. A.; Gast, A. P. *Phys. Rev. E* **1996**, *54*, 5447−5455.

(13) Ahn, J.-H.; Sohn, B.-H.; Zin, W.-C.; Noh, S.-T. *Macromolecules* **2001**, *34*, 4459−4465.
(14) Vaidya, N. Y.; Han, C. D.; Kim, D.; Sakamoto, N.; Hashimoto, T. *Macromolecules* **2001**, *34*, 222−234.
(15) Yokoyama, H.; Kramer, E. J. *Macromolecules* **2000**, *33*, 1871−1877.
(16) Yokoyama, H.; Kramer, E. J.; Hajduk, D. A.; Bates, F. S. *Macromolecules* **1999**, *32*, 3353−3359. Schaertl, W.; Tsutsumi, K.; Kimishima, K.; Hashimoto, T. *Macromolecules* **1996**, *29*, 5297−5305.
(17) Sato, T.; Watanabe, H.; Osaki, K.; Yao, M.-L. *Macromolecules* **1996**, *29*, 3881−3889.
(18) Watanabe, H.; Sato, T.; Osaki, K.; Yao, M.-L. *Macromolecules* **1996**, *29*, 3890−3897.
(19) Gohr, K.; Pakula, T.; Tsutsumi, K.; Schartl, W. *Macromolecules* **1999**, *32*, 7156−7165. Gohr, K.; Schartl, W. *Macromolecules* **2000**, *33*, 2129−2135.
(20) Choi, J.-H.; Ryu, J.-H.; Kim, S. Y. *J. Polym. Sci., Part B: Polym. Phys.* **2000**, *38*, 942−953.
(21) Ishizu, K.; Onen, A. *J. Polym. Sci., Part A: Polym. Chem.* **1989**, *27*, 3721−3731.
(22) Adams, J. L.; Graessley, W. W.; Register, R. A. *Macromolecules* **1994**, *27*, 6026−6032.
(23) Adams, J. L.; Quiram, D. J.; Graessley, W. W.; Register, R. A.; Marchand, G. R. *Macromolecules* **1996**, *29*, 2929−2938.
(24) Jack, K. S.; Wang, J.; Natansohn, A.; Register, R. A. *Macromolecules* **1998**, *31*, 3282−3291.
(25) Lai, C. Ph.D. Dissertation in Chemical Engineering; Princeton University, Princeton, NJ, 1999.
(26) Sebastian, J. Ph.D. Dissertation in Chemical Engineering, Princeton University, Princeton, NJ, 2001.
(27) Han, C. D.; Vaidya, N. Y.; Kim, D.; Shin, G.; Yamaguchi, D.; Hashimoto, T. *Macromolecules* **2000**, *33*, 3767−3780.
(28) Krishnamoorti, R.; Graessley, W. W.; Balsara, N. P.; Lohse, D. J. *J. Chem. Phys.* **1994**, *100*, 3894.
(29) Krishnamoorti, R.; Silva, A. S.; Modi, M. A.; Hammouda, B. *Macromolecules* **2000**, *33*, 3803−3809.
(30) Lin, C. C.; Jonnalagadda, S. V.; Kesani, P. K.; Dai, H. J.; Balsara, N. P. *Macromolecules* **1994**, *27*, 7769−7780.
(31) Schwab, M.; Stuhn, B. *J. Mol. Struct.* **1996**, *383*, 57−62.
(32) Kinning, D. J.; Thomas, E. L. *Macromolecules* **1984**, *17*, 1712−1718.
(33) Mortensen, K. *J. Phys.: Condens. Matter* **1996**, *8*, A103−A124.
(34) Percus, J. K.; Yevick, G. J. *Phys. Rev.* **1958**, *110*, 1.
(35) Ribbe, A. E.; Bodycomb, J.; Hashimoto, T. *Macromolecules* **1999**, *32*, 3154−3156.
(36) Leibler, L. *Makromol. Chem. Rapid Commun.* **1981**, *2*, 393−400. Mori, K.; Tanaka, H.; Hashimoto, T. *Macromolecules* **1987**, *20*, 381−393.
(37) Matsen, M. W. *Macromolecules* **1995**, *28*, 5765−5773. Vavasour, J. D.; Whitmore, M. D. *Macromolecules* **2001**, *34*, 3471−3483. Likhtman, A. E.; Semenov, A. N. *Macromolecules* **1997**, *30*, 7273−7278.
(38) Huang, C. I.; Lodge, T. P. *Macromolecules* **1998**, *31*, 3556−3565.
(39) Hadziioannou, G.; Skoulios, A. *Macromolecules* **1982**, *15*, 267. Tanaka, H.; Hashimoto, T. *Macromolecules* **1991**, *24*, 5713−5720. Zin, W.-C.; Roe, R.-J. *Macromolecules* **1984**, *17*, 183−188. Roe, R.-J.; Zin, W.-C. *Macromolecules* **1984**, *17*, 189−194.
(40) Yamaguchi, D.; Hashimoto, T.; Han, C. D.; Baek, D. M.; Kim, J. K.; Shi, A.-C. *Macromolecules* **1997**, *30*, 5832−5842.
(41) Hanley, K. J.; Lodge, T. P.; Huang, C.-I. *Macromolecules* **2000**, *33*, 5918−5931. Pedersen, J. S.; Hamley, I. W.; Ryu, C. Y.; Lodge, T. P. *Macromolecules* **2000**, *33*, 542−550.
(42) Kossuth, M. B.; Morse, D. C.; Bates, F. S. *J. Rheol.* **1999**, *43*, 167−196.
(43) Struglinski, M. J.; Graessley, W. W. *Macromolecules* **1985**, *18*, 2630−2643.
(44) Yrekli, K.; Krishnamoorti, R.; Tse, M. F.; McElrath, K. O.; Tsou, A. H.; Wang, H.-C. *J. Polym. Sci., Part B: Polym. Phys. Ed.* **2001**, *39*, 256−275.
(45) Plazek, D. J. *J. Phys. Chem.* **1965**, *69*, 3480.
(46) Graessley, W. W. In *Physical Properties of Polymers*, 2nd ed.; American Chemical Society: Washington, DC, 1993.
(47) Gell, C. B.; Krishnamoorti, R.; Kim, E.; Graessley, W. W.; Fetters, L. J. *Rheol. Acta* **1997**, *36*, 217−228. Tsenoglou, C. *J. Polym. Sci., Part B: Polym. Phys.* **1988**, *26*, 2329−2339.
(48) Leonardi, F.; Majeste, J. C.; Allal, A.; Marin, G. *J. Rheol.* **2000**, *44*, 675−692.
(49) Palierne, J. F. *Rheol. Acta* **1990**, *29*, 204−214. Palierne, J. F. *Rheol. Acta* **1991**, *30*, 497.

MA012024B